2007 IEEE International Conference on
Robotics and Automation
Roma, Italy, 10-14 April 2007

Automated Robot Docking Using Direction Sensing RFID

MyungSik Kim, Hyung Wook Kim, and Nak Young Chong

Abstract— **Automated target acquisition and docking is key to enabling various applications of autonomous mobile robots in indoor environments. For the purpose, many researches have been devoted to the development of location sensing techniques employing the latest in RFID or GPS. However, it has not yet become possible to attain high accuracy in those techniques, particularly in cluttered or dynamically changing environments. In this paper, we propose a novel location sensing RFID reader equipped with a dual directional antenna that communicates with controllable RF transponders. The dual directional antenna estimates the direction of arrival (DOA) of signals from various transponders by using the ratio of the received strength between two antennas. This enables the robot to continuously monitor the changes in the ratio and find its way to the target transponder. To verify the validity of the proposed system in real environments populated with unknown obstacles, we perform detailed experiments using simulations and hardware implementations. Specifically, the target acquisition and docking guidance are demonstrated in a multiple transponder environment under various circumstances.**

Index Terms— **RFID, DOA estimation, dual directional antenna, target acquisition, docking**

I. Introduction

One of the most common functions for autonomous mobile robots is to acquire a target and approach it for task execution. For this fundamental challenges in mobile robots, a location sensing RFID system was developed recently by the authors employing a single directional antenna to allow a robot to identify and approach an RF transponder [1], [2]. The system estimated the robot heading direction analyzing the pattern of the received signal strength transmitted from the target, whereby the robot could navigate toward the target. The results of the experimental test showed that the accuracy was within the reasonable range in an obstacle-free environment. However, in real environments, RF signals are easily distorted by obstacles that reflect and/or scatter the transmitting signal. This will result in incorrect direction finding, which hinders the authors from directly applying the proposed system to blind docking in real environments. Moreover, the previously developed system could sense only the stationary transponder, because it was required to repeat scanning the environment to estimate the DOA of the signal. The robot therefore could not detect changes in its surroundings while moving.

In this paper, we propose an enhanced location sensing RFID reader equipped with a dual directional antenna that interacts with controllable RF transponders. The proposed dual directional antenna system consists of two identical loop antennas perpendicularly positioned to each other having a 90° phase difference. It finds the DOA of signals by the ratio of the signal strength between two antennas without scanning the environment. Since the system can detect the changes in the DOA of the transmitted signal in real time, it can monitor the changes in target transponder location while keeping the robot moving around.

The proposed system and process for DOA estimation can straightforwardly be applied to location sensing based on bearing measurements, which features significant advantages over other localization approaches [3]. The vision based localization uses the location of targets identified from visual images. It therefore can sense the location with high accuracy, and the robot can detect its heading direction to the target from the image. But it requires the optical line of sight and the performances are often significantly affected by the environmental conditions such as changes in illumination [4], [5]. The range based approaches sense the location of the target using the distance estimated from the strength of RF signals or ultrasonic time of flight (TOF) measurements [6]–[8]. These approaches require multiple reference stations to trilaterate the position of the robot (or the transponder), but they cannot provide the direction of the heading of the robot. Thus, the robot should keep track of its heading direction while moving. However, since the proposed system identifies transponders on the fly and can keep the robot moving toward the target transponder along the estimated direction, it is highly useful for service robots in various applications.

This paper is organized as follows. In Section II, we briefly describe the fundamentals of electromagnetic theory underlying the measurement of the DOA. Section III shows the simulation results in using the DOA information for mobile robot navigation under different environmental conditions. In section IV, we show the experimental results that demonstrate the effectiveness of the proposed RFID system for target acquisition and docking. Finally, conclusions are drawn in Section V.

II. Estimation of the DOA

A. Dual Directional Antenna

As mentioned above, the location sensing is based on the bearing measurements that can be achieved by loop antennas exploiting their directionality. In this section, we provide a description of fundamental principles governing the DOA estimation with the dual directional antenna.

The dual directional antenna is a set of antennas consisting of two identical loop antennas perpendicularly positioned to each other. When an electromagnetic signal is transmitted to

This work was supported in part by Korea MIC and IITA through IT leading R&D Support Project.

The authors are with the School of Information Science, Japan Advanced Institute of Science and Technology, Japan {myungsik, hwkim, nakyoung}@jaist.ac.jp

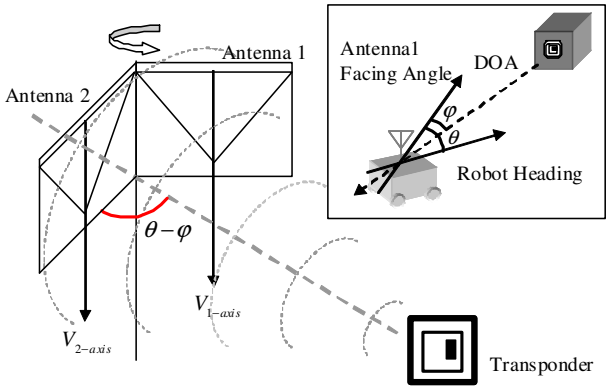

Fig. 1. Azimuth angle of the direction of arrival

the dual antenna as shown in Fig. 1, the voltages induced in each antenna corresponding to the received electromagnetic field can be expressed, respectively, as

$$V_1 \propto \left| \frac{CSB}{r} sin(\theta - \varphi) \right|,$$
$$V_2 \propto \left| \frac{CSB}{r} sin(\theta - \varphi + 90^\circ) \right|, \quad (1)$$

where S is the surface area of the antenna, B is the average magnetic flux density of the wave passing through the antenna, θ is the rotation angle of the antenna, φ is the bearing of the transponder, C accounts for the environmental conditions, and r is the distance from the transponder, respectively. Since the distance from the transponder will exceed one quarter wavelength, $\lambda/4$, for most applications, the voltage is inversely proportional to r [9]–[12].

Now we can obtain a dimensionless parameter defined as the ratio of the received signal strengths between two antennas given by

$$\nu_{12} = \frac{V_1}{V_2} = |tan(\theta - \varphi)|. \quad (2)$$

If we measure v_{12} and θ, the bearing of the transponder can be determined from Eq. 2.

Fig. 2 shows the patterns and the ratio of the received signal strength when the dual directional antenna in front of the transponder scans the environment from -90° to 90° with respect to its forward facing direction. Since the measured voltage may include an offset voltage as shown in Fig. 2(a), the magnitude of the strength ratio will change according to the actual working condition of the system. Thus, the accuracy of the DOA estimation from this ratio is somewhat limited, but is useful when the robot determines the direction of the approximate target heading.

In order to improve the accuracy of direction finding, we pay attention to three points of interest which are shown as the minimum, maximum, and crossover (or inflection) points in Fig. 2(b). The DOA estimation can be achieved relying on the fact that, while the ratio increases, the transponder can be located along the direction of the crossover point within the range bounded by the minimum and maximum points. Note that, however, the crossover points may be found twice in the area where the ratio increases if we also consider the remaining half of the environment, that is the backward facing direction of the antenna. The system therefore cannot distinguish between whether the detected transponder exists in front of the antenna or behind the antenna. In practice, the RFID system aims the antenna toward the target transponder by adjusting the antenna bearing to make the crossover point remain in the increasing area. Since the estimated DOA information is continuously fed to the robot, it can keep track of the transponder that moves at a reasonable velocity not exceeding the rotating velocity of the antenna.

It is experimentally confirmed that the accuracy of the DOA estimation using directional antennas is within $\pm 4^\circ$ in an empty indoor environment [2]. However, since the signal may be easily distorted by the environmental condition, the estimated DOA may be shifted toward or away from the obstacle in the environment. To estimate the amount of shift, we need to know the exact condition of the environment such as reflexibility or transmittance of the objects and walls (or partitions). Thus, it is almost impossible to estimate exactly the DOA in a cluttered environment. However, we can estimate the amount of shift in the DOA information

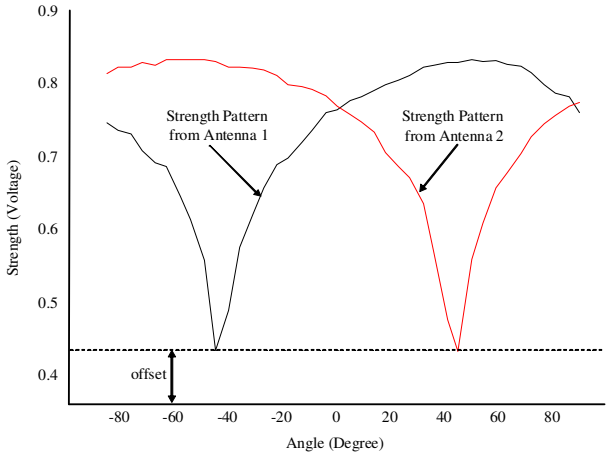

(a) Signal patterns

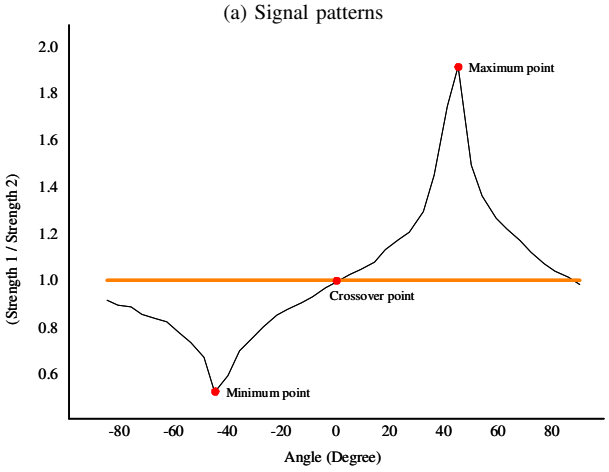

(b) Signal ratio

Fig. 2. Patterns and ratio of the received signal strength

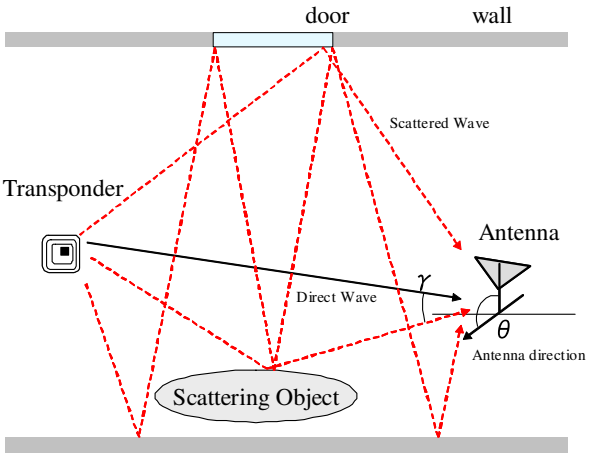

Fig. 3. Multi-path propagation in real environment

within an error range by imposing reasonable assumptions.

B. DOA estimation in cluttered environments

The total electromagnetic wave transmitted from a transponder is the sum of the direct wave and the scattered waves as shown in Fig. 3 [13], [14]. Thus the total wave arrived at the antenna can be given as

$$F_{Total} = F_{direct} + \sum_{i=1}^{n} F^{\,i}_{\,scattered}. \tag{3}$$

By substituting $B = B_0 \sin(\kappa r - \omega t)$ into Eq. 1, the wave can be expressed as

$$F = \frac{CSRB_0 \sin(\kappa r - \omega t)}{r} \sin(\theta - \varphi), \tag{4}$$

where B_0 is the magnetic flux density of the transponder, R is the coefficient of the strength of the arrival signal ($R = 1$ when the wave is the direct wave), κ is the propagation vector, ω is the frequency of the transmitted wave, φ is the angle of incidence of each transmitted wave, and r is the traveling distance of the wave, respectively [13], [14]. In the equation, the first term of the sine reflects the properties of the transmitted signal and the second term of the sine accounts for the change in the received signal strength according to the antenna facing angles.

Assuming that the direct wave and the scattered waves have the differences in the angle of incidence, γ_i, and the traveling distance, Δr_i, respectively, the right-hand side of Eq. 3 can be expanded as

$$\frac{CSB_0 \sin(\kappa r_0 - \omega t)\sin(\theta - \varphi_0)}{r_0} + \frac{CSR_1B_0 \sin(\kappa r_0 - \omega t + \frac{2\pi\Delta r_1}{\lambda})\sin(\theta - \varphi_0 + \gamma_1)}{r_0 + \Delta r_1} + \ldots, \tag{5}$$

where r_0 is the traveling distance and φ_0 is the angle of incidence of the direct wave. In Eq. 5, the direct wave and the scattered waves have a phase difference of $2\pi\Delta r_i/\lambda$ due to the difference in traveling distances, Δr_i.

To see the effect of the scattered wave, the phase shift in the measured direction is examined. Denoting all terms except $sin(\theta - \varphi_0 + \gamma_i)$ as a_i and $(\theta - \varphi_0)$ as χ, Eq. 5 can be rewritten as

$$a_0 \sin(\chi) + a_1 \sin(\chi + \gamma_1) + \ldots \quad . \tag{6}$$

Again Eq. 6 can be expanded as

$$a_0 \sin(\chi) + a_1 \cos(\gamma_1)\sin(\chi) + a_1 \sin(\gamma_1)\cos(\chi) + \ldots \quad . \tag{7}$$

Using the sum formula for sine, Eq. (7) can be transformed into

$$F_{Total} = A \sin(\chi + \eta) \tag{8}$$

where

$$A = \left[\left(\sum_{i=0}^{n} a_i \cos(\gamma_i) \right)^2 + \left(\sum_{i=0}^{n} a_i \sin(\gamma_i) \right)^2 \right]^{1/2},$$

$$\eta = \tan^{-1} \left\{ \sum_{i=0}^{n} a_i \sin(\gamma_i) / \sum_{i=0}^{n} a_i \cos(\gamma_i) \right\}.$$

In Eq. 8, η is the phase shift in the total field cause by the effects of the scattered waves and it represents the potential error in estimated direction. It is now straightforward to rewrite η as

$$\eta = \tan^{-1} \left\{ \frac{\sum_{i=0}^{n} \frac{R_i \sin(\gamma_i)\sin(\chi + \Phi_i)}{r_0 + \Delta r_i}}{\sum_{i=0}^{n} \frac{R_i \cos(\gamma_i)\sin(\chi + \Phi_i)}{r_0 + \Delta r_i}} \right\}. \tag{9}$$

The numerator and denominator of the argument in the arctangent are expressed as the sum of $\sin(\chi)$ with the magnitude of $\frac{R_i \sin(\gamma_i)}{r_0 + \Delta r_i}$, $\frac{R_i \cos(\gamma_i)}{r_0 + \Delta r_i}$, respectively, and the phase difference of Φ_i.

When multiple waves arrive at the same time, the magnitude and phase of one wave are interfered by the other waves. And the magnitude of waves are increased or decreased by the differences in phase among waves. In Eq. 9, the element of the direct wave in the numerator is zero, then the magnitude of the denominator becomes bigger than the numerator by the direct wave term. Thus, even though η is added, the estimated direction still points the direction to the target. And the effect of the direct wave increases as the robot moves closer to the transponder, then η becomes zero. Also, the effect of the static field increases near the transponder. The signal strength therefore increases rapidly when the robot comes into proximity with the transponder, which enables the robot to find itself located at the target.

III. Simulation of DOA Guided Navigation

A. Conditions for the Simulation

To verify the validity of the proposed system, we performed experiments of autonomous navigation using the simulator developed in-house. Fig. 4 shows the layout of the simulation program. In Fig. 4, Part (a) shows the simulation environment including a robot, a transponder, walls, and obstacles. The number of obstacles and the location of the

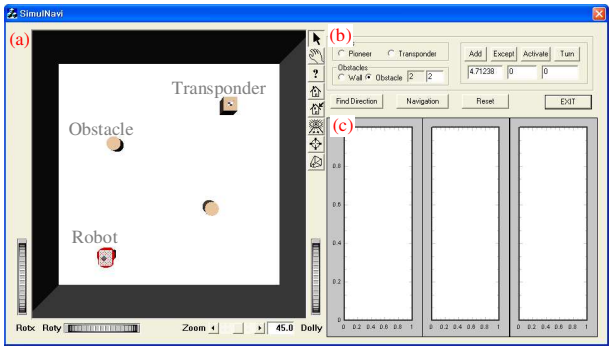

Fig. 4. Layout of simulation program

robot can be modified by the control panel in Part (b). The path of the robot is displayed in Part (a) and the desired target direction, the estimated direction, and the estimation error are displayed in Part (c). Since it is almost impossible to include the whole scattering effect of signals in the obstacle cluttered environment, we implemented the basic ray-tracing principle explained in the previous section.

The conditions used in the simulation are as follows.

- A transponder is considered as a point charge.
- The scattering of the signal by an obstacle is assumed to be occurred at the center of the obstacle, not the surface.
- All obstacles scatter signals with randomly determined rates R_i. Obstacles that do not affect transmission of signals are not included.
- The size of the room is 5m×5m.
- The operating frequency is 303.2MHz.
- The robot is considered to receive signals associated with far-field regions, since the 50cm radius of the transponder (or the goal) location exceeds $\lambda/4$.
- The strength of the multiple-scattered signal is small enough to be ignored.
- Intrinsic sensing error of $\pm 4^\circ$ with the gaussian distribution is included in estimating the DOA.

The robot navigates according to the following steps.

1) The robot scans the transmitted signal from -90° to 90° and estimates the DOA of the signal source by the minimum, maximum, and crossover points on the signal ratio curve.
2) The robot moves 30cm in the estimated DOA that is continuously corrected by keeping the ratio remained at the crossover point.
3) If the distance measured from the strength becomes less than 50cm, then the robot stops moving.

B. Simulation Results

Simulations were performed under four different conditions. The simulation results are shown in Fig. 5. In each figure, the left part displays the location of the obstacles and the movement of the robot. The right-hand side graph shows the changes in the direction to the target transponder (black solid line with dot), estimated direction (red dash-dotted line with square dot), and direction sensing error caused by the movement of robot (blue dotted line with diamond dot).

Fig. 5(a) shows the navigation result in the obstacle-free space. Since the signal is transmitted without scattering, the robot moved straight toward the transponder. The error is within the intrinsic accuracy of $\pm 4^\circ$.

When the environment is enclosed by the solid walls as shown in Fig. 5(b), the error increased. However, the direct wave became dominant as the robot moved closer to the transponder. Thus, the error decreased gradually.

In Fig. 5(c), several obstacles were located between the robot and the transponder. The signal wave was scattered by the obstacles, but was not totally blocked. Thus, the robot could search for the propagated signal. While the robot navigated, the error increased or decreased according to the changes in the object location with respect to the robot position. However, the error became smaller, as the robot moved away from the obstacles.

Fig. 5(d) shows the result when the transponder was located behind the antenna. As explained in section II, the proposed system can not distinguish between whether the transponder exits in front of the antenna or behind it. When the transponder exits behind the antenna, the DOA estimation may include the error of about 180°. However, we can cope with this potential error, since it is evident that the received signal strength increases as the robot approaches the transponder. This means that if the robot does not move in the wrong direction, the signal strength will increase. Thus, if the signal strength decreases while robot navigates, it needs to turn 180° around to find the correct direction as shown in Fig. 5(d). The remaining process is the same as the previous cases.

IV. Experimental Results

A. Experimental Setup

Fig. 6 shows the developed RFID-enabled self-navigating and docking mobile robot system. The system is composed of two parts: 1) a location sensing RFID reader interacting with the controllable transponders and 2) a mobile robot equipped with the proposed RFID reader. The robot is controlled by the server PC and the operator can access the robot through the client PC with wireless communication. The server PC controls the RFID system as well and identify transponders in the environment. The reader can control the activation of the transponder and read the information encoded in the transponder. In this experiment, the transponders are selectively activated by the reader after being identified.

B. Experiment Results of Self-navigation

To verify the performance of the proposed RFID system in a real environment, we built an experimental environment as shown in Fig. 7 that includes a Pioneer 3-DX equipped with the RFID reader and three transponders of a kind. After the robot and the RFID system are initialized, all transponders that exist in the environment are identified. Once one of the transponders is activated by the operator, then the robot moves to that transponder. The RFID reader keeps track of the direction to the transponder and informs the direction to the robot on demand. The robot stops

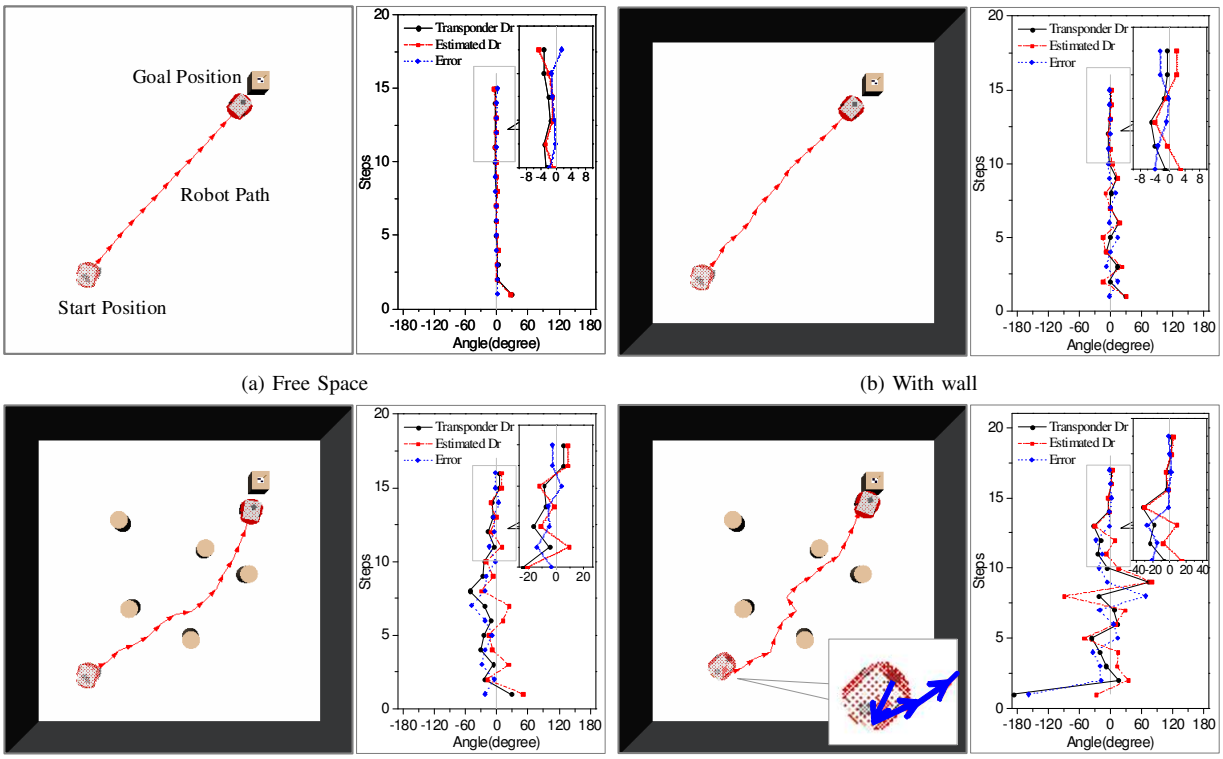

(a) Free Space (b) With wall

(c) With wall and obstacles (d) Transponder behind the antenna

Fig. 5. Simulation Results

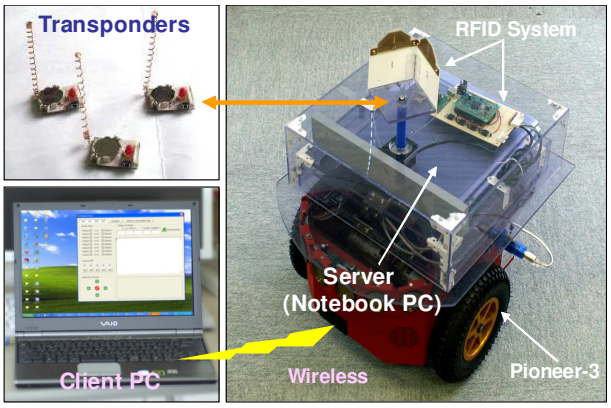

Fig. 6. System setup

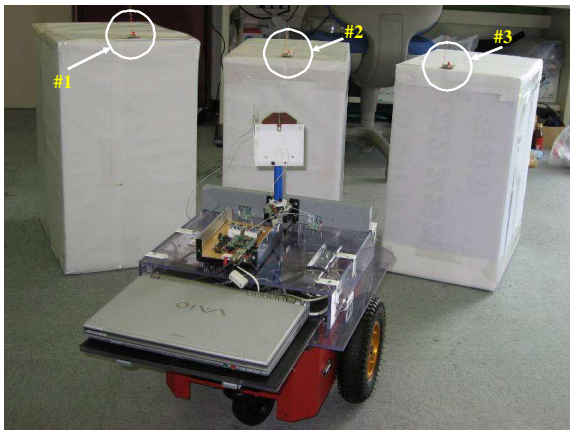

Fig. 7. Snapshot of experiment

approaching the transponder when the transponder is within the distance range of 30cm from the robot or the signal strength is higher than a pre-specified value. On the basis of the above scenario, we performed four sets experiments in an electromagnetically hostile environment.

Fig. 8 shows the image of a virtual environment that displays the experimental results. Three transponders are located at (0, 2)m, (-1.5, 1.5)m, (1.5, 1.5)m with respect to the initial robot position in Cartesian coordinates. The trajectories of the robot are displayed as dots in this environment.

Fig. 9 shows the experimental results of robot docking guided by the DOA estimation. Fig. 9(a) shows the results of three sets of experiments. The robot identified three transponders and approached the target transponder activated for each trial. Comparing to the other results, the path for the transponder at (-1.5, 1.5)m was deviated from a straight line. In this case, the received signal was distorted to some degree by the object located close to the path. However, the robot kept adapting the direction of its heading and could finally reach the target.

Fig. 9(b) shows the result when a person stands in front of the robot and chairs are positioned between the robot and the target. Since the obstacles scattered the signal, the estimated DOA gave incorrect directions when the robot found its way around the obstacles. However, notable observation we

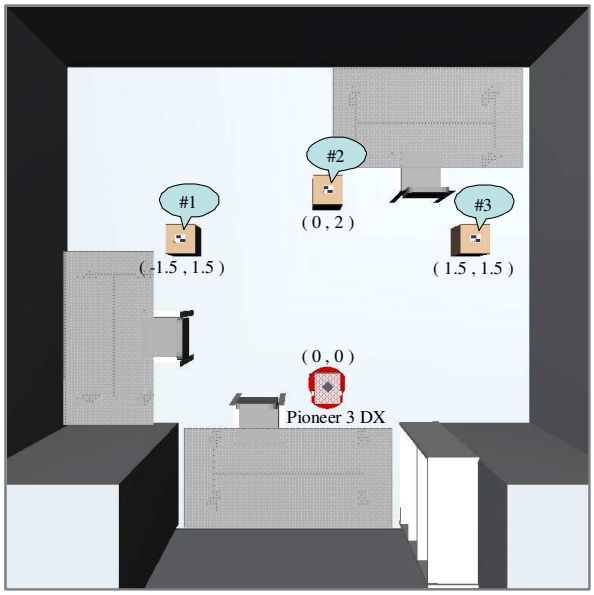

Fig. 8. Virtual environment for displaying experimental results

made is that the deflected signal path led the robot not to collide with those obstacles. This feature does not hold for the obstacles through which the signal passes, but it is still useful when the robot self-navigate in the real environment populated with obstacles.

V. Conclusion

We proposed a direction finding RFID system that enabled automated robot docking to a specific target in a cluttered indoor environment. The robot equipped with the proposed system found its way to the target using the DOA estimation by the ratio of the signal strength received at the dual directional antenna. Our major contributions can be summarized as: 1) The proposed RFID system can find the direction of the target in real time without scanning the environment. 2) The DOA guided docking has proven to be robust and reliable to a wide range of signal distortions.

Based on the good agreement between the experimental results and theoretical predictions, we can confirm that the robot will be able to self-navigate toward the target transponder avoiding the obstacles that occlude the path to the target. Our future effort includes the recovery of the distorted signals for efficient localization of transponders and the enhancement of self-navigation with other aiding sensors.

References

[1] M. Kim, T. Kubo, T. Tsunenori, and N. Y. Chong, "Location Sensing Algorithms for Active RFID," *JSME Robotics and Mechatronics Conf.*, 2A1-N-054, 2005

[2] M. Kim and N. Y. Chong, "RFID-based Mobile Robot Guidance to a Stationary Target," *Mechatronics*, Elsevier Science Ltd., Accepted.

[3] J. Hightower and G. Borriello, "Location Systems for Ubiquitous Computing," *IEEE Computer Magazine*, Vol.34, No.8, pp.57-66, 2001.

[4] D. C. K. Yuen and B. A. MacDonald, "Vision-Based Localization Algorithm Based on Landmark Matching, Triangulation, Reconstruction, and Comparison," *IEEE Transactions on Robotics*, pp.217-226, 2005

[5] S. Se, D. G. Lowe, and J. J. Little, "Vision Based Global Localization and Mapping for Mobile Robots," *IEEE Transactions on Robotics*, PP.364-375, 2005.

[6] A. Smith, H. Balakrishnan, M. Goraczko, and N. Priyantha, "Tracking Movign Devices with the Cricket Location System," *Proc. of the 2nd Int. Conf. on Mobile systems, Applications, and Services*, pp.190-202, 2004.

[7] J. Hightower, G. Borriello, and R. Want, "SpotON : An Indoor 3D Location Sensing Technology Based on RF Signal Strength," *UW CSE Technical Report*, Feb. 18, 2000.

[8] L. M. Ni, Y. Liu, Y. C. Lau, and A. P. Patil, "LANDMARC : Indoor Location Sensing Using Active RFID," *ACM Wireless Networks*, Vol.10, No.6, pp.701-710, 2004.

[9] J. R. Reitz, "Fundations of Electromagnetic Theory," *Addison Wesley*, 1993.

[10] D. M. Pozar, "Microwave and RF Wireless Systems," *Wiley Text Books*, 2000.

[11] W. L. Stutzman and G. A. Thiele, "Antenna Theory and Design," *John Wiley & Sons Ltd.*, 1999.

[12] C. A. Balantis, "Antenna Theory: Analysis and Design," *Wiley Text Books*, 1996.

[13] F. A. Alves, M. R. L. Albuquerque, S. G. Silva, and A. G. d'Assuncao, "Efficient Ray-Tracing Method for Indoor Propagation Prediction," *SBMO/IEEE MTT-S Int. Conf. on Microwave and Optoelectronics*, pp.435-438, 2005.

[14] L. Tsang and J. A. Kong "Scatterning of Electromagnetic Waves : Advanced Topics," *John Wiley & Sons Ltd.*, 2001.

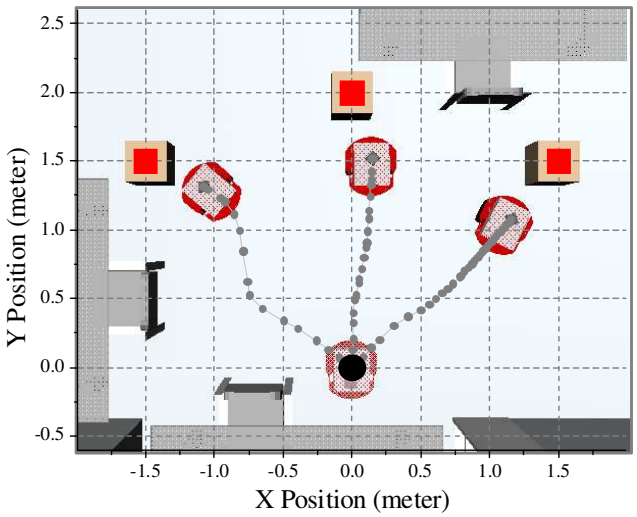

(a) approaching a target among three transponders

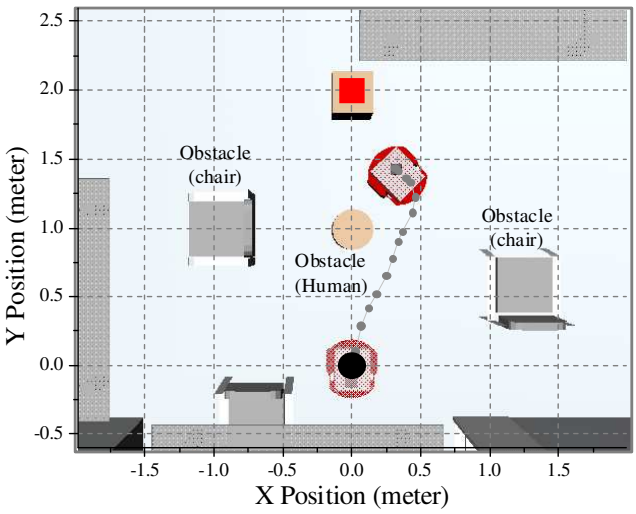

(b) approaching a target while a person blocks the way to the target

Fig. 9. Experiment Results